Materials Science Forum
ISSN: 1662-9752, Vol. 1002, pp 161-174
doi:10.4028/www.scientific.net/MSF.1002.161

Submitted: 2020-02-02
Revised: 2020-03-06
Accepted: 2020-03-06
Online: 2020-07-14

Erosion-Corrosion Behavior of Al-20%Ni-Al_2O_3 Metal Matrix Composites by Stir Casting

Nawal Mohammed Dawood

College of Materials Engineering- Metallurgical Engineering department, Babylon University

Mat.newal.mohammed@uobabylon.edu.iq

Keywords: Metal matrix composite, Stir casting, Corrosion, NiAl, Erosion-corrosion

Abstract. As a matrix, aluminum has been widely studied because of its wide range of applications and outstanding properties. Scientists of material science usually face some challenges regarding mechanical and tribological properties of aluminum because of its poor behavior with respect to these aspects. Therefore, the main objective of this work is to enhance the corrosive resistance and mechanical properties of aluminum by strengthening it by addition of nickel and aluminum oxide through stir casting by using the vortex technique. Al-Ni-Al_2O_3 composition was prepared by adding a fixed value of Ni (20%) and mixed with different values of Al_2O_3 for a range of (4-8%) within 2 wt.% increment. Vortex technique was used for the stir casting required for the composite material preparation. It is noted that increasing of Al_2O_3 percentage increases the hardness of the composite of the aluminum matrix. The maximum increment of the hardness values (about 55%) was found at 8% Al_2O_3 composite. The erosion-corrosion, general corrosion for the alloy of Al-20%Ni base, and the prepared composite material were achieved within 3.5wt% NaCl solution used as a corrosive medium for the general corrosion. Whereas, for the erosion-corrosion at 90° as the impact angle, the slurry solution (1wt%SiO_2 sand in 3.5wt% NaCl solution as the erodent) was used. It was noted that, the rate of the general corrosion of the specimen of the composite is smaller than that corresponding of the base alloy (Al-20%Ni). Regarding the results of the erosion-corrosion, the resistance of erosion-corrosion of the composite was enhanced considerably with increasing Al_2O_3 percentages values. A noticeable improvement in the resistance of corrosion of the aluminum composite as compared to the pure aluminum specimen was noticed due to effect of nickel addition. However, the rate of corrosion was declined with increasing the percentage of Al_2O_3. The great reduction of the this rate was 26% (measured by mpy) noticed at 8% Al_2O_3 composite. In addition, this value was smaller than that corresponding for the base alloy.

Introduction

The main advantage of the composite material is the developing of new materials with new properties. The developed composite materials show highly unrelated (dissimilar) properties as compared to the properties of main components individually. The conservative materials either present high density and high strength, however its workability is low, or it show high ductility and machinability, but its wear resistance is small [1]. In other words, the individual materials show both good and bad properties simultaneously. People tried to create new materials that show the preferable and desirable properties where effect of undesired properties can be eliminated. The only way to get these outwardly properties is by creating and developing what called composite materials [2]. In general, composite materials can be developed to provide higher stiffness to weight ratio, higher strength to weight ratio, higher resistance for fatigue, higher wear resistance [3], improved thermal properties and corrosion resistance. The advantages of composite materials have encouraged people to use these materials in different industrial applications [4, 5]. Composite materials become the direction that people head to develop unique materials within unique properties. Composite materials are more common for all kind of the real live applications due to its flexibility and ability to be custom-made to provide specific properties.

Choosing of matrix material for developing specific composite materials depends on requirements of the application. For example, the light materials used as matrix can be processed easily, such as iron, steel, copper, aluminum. In this work, pure aluminum was used as a matrix due to its workability and its easy processes. Aluminum is the material that widely used in several engineering applications due to its good properties, such as high strength, low weight, low density, high electrical and thermal conductivities [6] , high resistance against corrosion [7], and its easy availability. In addition, aluminum composite and its alloys are using in automobiles applications [8, 9], nanotechnology, marine applications, MEMs, space technologies, aircrafts, and MMCs [10]. The Erosion-corrosion process is a complex degradation and severe process in which the electrochemical and mechanical events interact each other producing material properties loss and then component failure [11]. The main reason of losing the principal material properties is the effect of degradation of the of the properties of the individual mechanical and electrochemical components by a term called additives effect or synergistic or [11, 12]. Numerous industrial processes are detrimentally influenced by erosion-corrosion. For examples, the process of oil sands extraction [13-15], power generation [16], production of phosphoric acid [17], mineral and metal extraction [18], and acidic latching process of some industrial minerals, for instance silicate, copper, and phosphate rocks and others. The erosion damage for an erosion-corrosion process is developed from impacting of solid particles on the surface of material at different velocities and angles. It is worthy to mention that the extent of the damage and erosion mechanism depends on the impact conditions and materials mechanical properties [19-21]. For example, the impact energy is absorbed when the target material is ductile due to its elastic and plastic deformations, hereby, debris and material lip are shaped and gradually removed by successive impact [22]. However, the impact energy is dissipated when the target material is brittle, because of the micro-crack formation and growth beside the accompanied micro-fatigue. The presence networks of micro-crack merges material fracturing and produces material loss [23].

Several studies have been accomplished for understanding the influences of corrosion on the degradation of material in the presence of erosion-corrosion conditions. For example, some scientists recommended that for the active materials, the layer of the work-hardened and debris of the material formed by erosion were removed by the anodic dissolution [11]. Furthermore, increasing of the surface roughness resulted from the plastic deformation that enlarging material surface area that exposed to the erosion-corrosion effect. Xie et al. [24] stated that the strain energy of surface for high carbon and low-alloy steel increased as a result of successive mechanical erosion. It was found that the strain energy enhanced the steel surface anodic dissolution along with increasing its potential of corrosion toward the active values [24]. The protective layers of the passive materials can be actually eliminated or removed by the impacts of solid particles [25-28]. In general, the re-passivation and de-passivation processes are in a competition. In other words, if the surface is exposed to a severe and continuous degradation in erosion, a specific layer of that surface will be removed, and the uncovered or unprotected surface is going to be subjected to an aggressive media [25, 28].

Corrosion of the multiphase material, such as metal-matrix composite (MMCs), could dissolve the matrix phase and rigid phase-matrix interface [12, 29]. The severity and intensity of the dissolution depend on the resistance against corrosion of the matrix phase, the difference in the electrochemical potential of corrosion (Ecorr) of the hard phase and the matrix, and the presence of additional precipitate [30, 31]. The current research aims to enhance both mechanical properties and resistance against corrosion of the aluminum after strengthening it with nickel and aluminum oxide by preparing specimens of aluminum-nickel-aluminum oxide composite materials in a way of manufacturing stir casting where the percentage of nickel is fixed at 20 wt.% with different weight percentages of aluminum oxide (4-6-8 wt.%). Further, the erosion-corrosion behavior of all composites in seawater (3.5% NaCl solution) and slurry solution with 1wt% SiO_2 sand in seawater was investigated.

Experimental Work

Preparation of Al-20wt.% Ni Specimens

The aluminum samples were put into the crucible made from graphite which and then they was placed inside the electrical furnace. Using thermocouple type-k, the temperature change inside the

crucible was monitored. The furnace temperature was raised up to 750˚C for reaching the liquid temperature required to melt the aluminum entirely. The argon stream was applied on the **molten charge** to take out the slag on the surface and removing it via an alumina spoon. Then, nickel flakes were added gradually and stirred until it melted. Subsequently, the molten charge was poured into the steel die. The steel was well-dried prior the casting process at a temperature equal to 200ºC utilizing the drying instrument. The casting was then left to cool down at room temperature. Finally, the alloy specimens with a diameter equal to 10 mm and a height equal to 90 mm were prepared.

Preparation of Al-20wt.% Ni – Al_2O_3 Composites Specimens by Stir Casting

The stir casting technique was used to prepare composite specimen. In this experiment, a prepared alloy (Al-20%Ni) was first chopped into small pieces for easier melting inside the furnace. It was then superheated above the liquids temperature to create a vortex in the melt using a graphite stirrer. An electrical stirrer was used to mix the Al_2O_3 particles (size of 75μm) with the molten Al-20%Ni alloy and in the production of Al_2O_3 particles reinforced Al-20%Ni matrix composites. Al_2O_3 particles (4, 6, 8 wt%) were wrapped in high-purity aluminum foils and heated to 300°C for 60 minutes in the heating furnace. The heated Al_2O_3 particles were added to the molten Al-20%Ni alloy and ring the mixture was stirred for five minutes at a speed of 500rpm. Then, the molten was poured into a pre-heated steel mold to 200°C by gravity casting. Finally, the alloy specimens with a diameter equal to 10 mm and a height equal to 90 mm were prepared.

Heat Treatments

The heat treatment was conducted at a temperature of450˚C for 6 hours in order to homogenize the composition, eliminate the semi-soluble phases, and ensure that the casting elements and impurities were homogenously distributed in the alloy, giving the alloy hardness and homogeneous mechanical properties.

Specimen Preparation for Microstructure

The specimens made from the prepared composites of Al -20% Ni/4, 6, and 8 %Al_2O_3 and base alloy were ground, polished, etched and then observed by an optical microscope in sequence steps. Different grits of SiC emery clothes (220, 320, 500, and 1000) were used in the presence of water for the grinding operation. The process of polishing was conducted by means of the diamond paste having a size equal to 1μm, lubricants, and a special polishing cloth. Water and alcohol were used to clean the sample and then dried using hot air. The samples etching process was performed with the help of an etching solution contains (99% H_2O+1% HF)[32]. Finally, water and alcohol were used to wash the samples and left to dry. Scanning electron microscopy examination of specimens was performed.

Hardness Test

Hardness test was performed in accordance with ASTM E10 standard. A ball identer made from hardened steel with a diameter equal to 10 mm in this test. The subjected load was 500 kgf according to [33] procedure. The indent diameter was then measured across the perpendicular direction. The average diameter of three indents were considered.

Corrosion Tests

Experimental Media

Two media were used in this work, the first was seawater of 3.5 wt% NaCl solution for general pure corrosion test at room temperature (25°C) and the second slurry media was a mixture of 1 wt% SiO_2 sand with 3.5 wt% NaCl solution for erosion-corrosion test at 25 ℃, the particle size ranges were 53-350 μm.

The pure corrosion and erosion-corrosion tests conditions are shown in the Tables (1 and 2) under the influence of some parameters such as pH and flow rate at a constant temperature equal to 25°C and a pressure of the media equal to 1 bar**.**

Table 1: General pure corrosion test conditions.

Type of the Medium	Single – Phase :(Corrosive Medium)
Temperature (º C)	25
Medium Pressure (bar)	Zero (Static Medium).
Flow Rate (Q) (l/min)	Zero (Static Medium).
pH	8.2

Table 2: Erosion – corrosion test conditions.

Type of the Medium	Two-Phase: 1 wt% silica sand as slurry (Erosive Medium) and Sea water (Corrosive Medium)
Temperature (º C)	25
Medium Pressure (bar)	1
Flow Rate (Q) (l/min)	36
pH	8.2

Specimens Preparation for Corrosion Test

The specimens were machined and transformed into pieces having circle cross section of 10 mm diameter and 5 mm thickness for the immersion test or the weight loss method. The specimens were ground or abraded in sequence on 180, 220, 320, 500, and 1000 grades with emery paper of SiC and water for cooling the specimens. Then, the specimens were polished using special cloth with alumina (Al_2O_3) suspension of particles size of 0.5μm in solution. The specimens were washed with water and alcohol, dried in hot air, and kept in a desecrater.

Electrochemical Test

Most corrosion in metals occurs on the boundary located between the electrolyte solutions and metals during the electrochemical reactions. The test of corrosion resistance in 3.5% NaCl solution was conducted using the electro-chemical method; where, the corrosion rate was calculated for several samples. Firstly, every specimen has subjected to open circuit potential. Following this, the current of anode and cathode were measured nearly this potentials. The relationship between of the current (logarithmic scale) vs electrode potential, named Tafel Plots, was constructed. The corrosion currents were found by extrapolating the anodic and cathodic linear regions of the curves. The corrosion rate were calculated on the basis of the following equation [34]:

$$\text{Corrosion rate(mpy)} = 0.13\, I_{corr}\, (E.W)\, /\rho \quad (1)$$

Where:

E. W= equivalent weight (g/eq.)

ρ= denotes the density (g/cm³)

0.13 = metric and time change factor

icorr. = corrosion current density (μ A/cm²).

mpy = Corrosion rate (mils per year)

Erosion-Corrosion Test Apparatus

Fig. 1 shows the schematic diagram of an erosion-corrosion device. The erosion-corrosion apparatus was designed and constructed according to the standard test apparatus that explained in American Standard (ASTM G73).

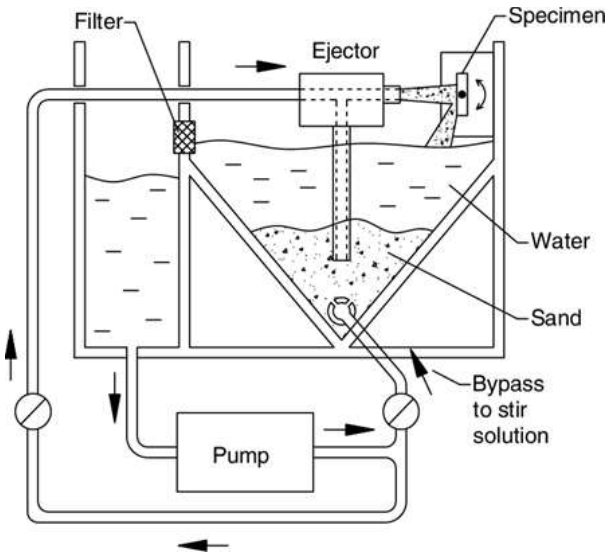

Fig. 1: A schame of the erosion-corrosion device [35].

Results and Discussions

Chemical composition of the prepared specimens

Tables 3 demonstrate the chemical compositions of the Al-20 wt% Ni

Table 3: Chemical compositions of Al-20 wt% Ni.

Element%	Ni	**Si**	**Fe**	**Cu**	**Mn**	**Mg**	**Zn**	**Cr**	**Ti**	**Sn**	**Pb**
	18.113	1.35	0.498	0.555	0.175	0.254	0.447	0.0527	0.0687	0.500	0.253
	Al	**V**	**Bi**	**Zr**	**B**	**Ga**	**Cd**	**Co**	**Ag**	**In**	**Ce**
	Bal.	0.0476	0.650	0.0614	0.0250	0.0644	0.350	0.304	0.118	0.150	0.0500

Microstructure of Prepared Specimens

Fig. 2 shows the SEM images for etched Al-20%Ni with different magnification while Fig. 3 shows the EDS Spectrum analyses for Al-20%Ni alloy. Fig.4 shows the SEM images for etched Al-20%Ni-8% Al_2O_3 with different magnification while Fig. 5 shows EDS Spectrum analyses for Al-20%Ni-8% Al_2O_3 alloy. The existence and distribution of the main alloying elements aluminum, nickel, oxygen is clear at the pointed region. The microstructures exhibited an increase in the reinforcements content within the matrix and suggested that the distribution was uniform. Moreover, the structure of the grain seemed to be equiaxed.

X-ray Diffraction (XRD) Test

The technique of XRD is important to identify the phases of crystalline structure. Figures 6 and 7 show the XRD patterns for Al-20%Ni and Al-20%Ni -8%Al_2O_3 alloy respectively. It can be observed that Al, Ni has transformed to (Al_3Ni_2) phase.

Hardness Test

In this work, the Brinell hardness values of all alloys were measured and the results are illustrated in Fig. 8. The maximum value was identified for B3 samples with 8% Al_2O_3, that is attributed to the relatively high hardness value of Al_2O_3 particles itself which obstructs the dislocation movement [36].

The increment percentage of Brinell hardness is 27%, 46% , 52% for B1, B2, and B3 specimens, respectively, when compared with sample A. These results are in good agreement with the results obtained in reference [37] with a small difference due to using different reinforcement types and average particle sizes of Al_2O_3.

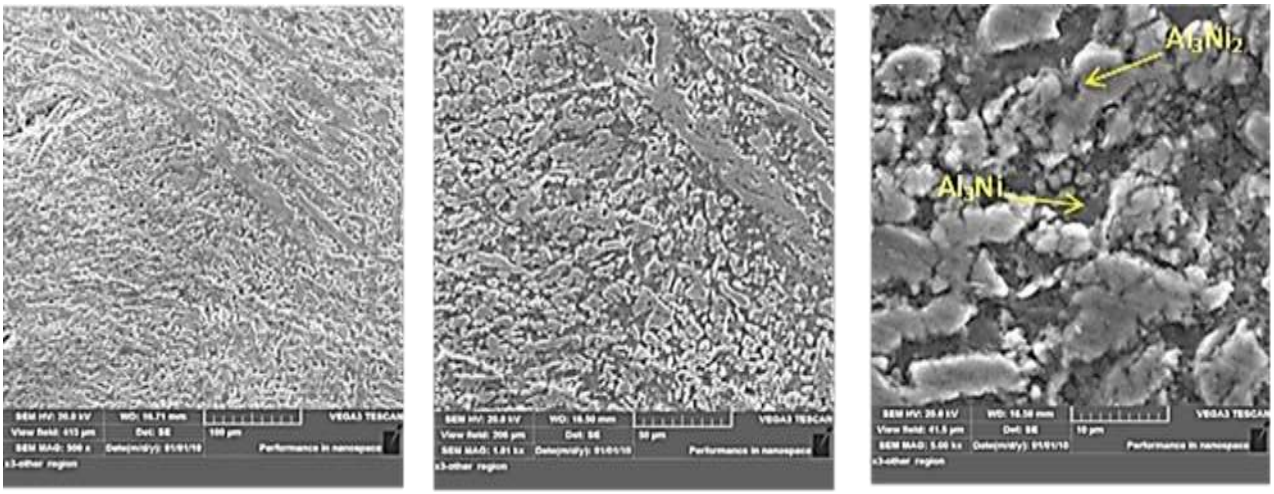

Fig. 2: SEM images of etched Al-20%Ni alloy with different magnification

General Pure Corrosion Results

Fig. 9 indicates the results of weight loss rate in the general pure corrosion of base (Al-20%Ni) and composite specimens in 3.5wt% NaCl after the immersion time of 20 hours at a 2-hour cycle. It was seen that the rate of weight losing in unit (g/cm2) increases continuously with the immersion time because of the removal of surface layer and oxide, and the formation of new surface exposed to corrosion. The composite specimen has the lower weight loss rate than that of base alloy after different immersion times. This is due to the presence of the hard phase of Al2O3 particles which are uniformly distributed in the microstructure of Al-20%Ni alloys. These particles improve the microstructure and increase the hardness of base alloy.

Fig. 10(a) shows the micrograph of base alloy (Al-20%Ni) which is the metal surface exposed to pure corrosions in 3.5% NaCl solutions, pits are seen on the surface resulting from pitting corrosion with chloride ions. This is due to the breaking of oxide film which is porous and non-adherent as indicated by Shreir [38]. Fig. 10(b) shows the micrograph of composite sample (Al-20%Ni - 8%Al2O3) which seems free from pits.

Electro-chemical Test

Fig. 11 illustrates polarization curves for the Al-20%Ni alloy and composite specimens in 3.5%NaCl solution. The corrosion current could be found by converting the log currents scale into actual values. It should be noticed that there is an important shift toward lower current densities of the polarization curves for composites with different Al_2O_3 particulates. For example, Al-20%Ni corrosion current density is around 0.6731µA/ cm^2 while for 4% Al_2O_3 is about 0.4632 µA/ cm^2 and for 6% Al_2O_3, it is about 0.0765 µA/ cm^2 but at 8% Al_2O_3, the corrosion current density is 0.0150 µA/ cm^2. Further, it can be seen the highest improvement percentage is 97% when the concentration of Al_2O_3 particulates is 8%. These outcomes specify stable behavior of Al-20%Ni-Al_2O_3. The corrosion rates (mpy) of the different specimens are shown in the Fig. 12; while, Table 4 illustrates the corrosion potential (Ecorr.) and Corrosion Current (icorr.) of Al-20%Ni with and without Al_2O_3 in 3.5% NaCl.

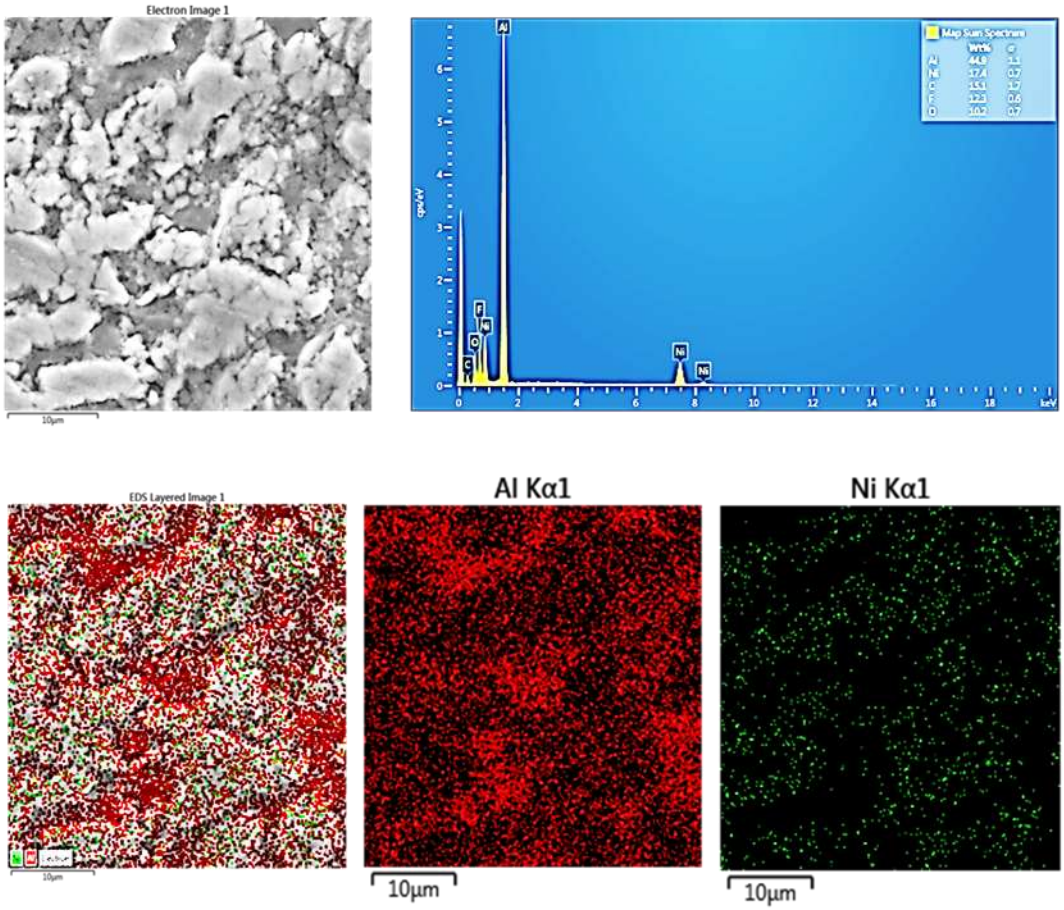

Fig.3: EDS Spectrum analyses of Al-20%Ni alloy.

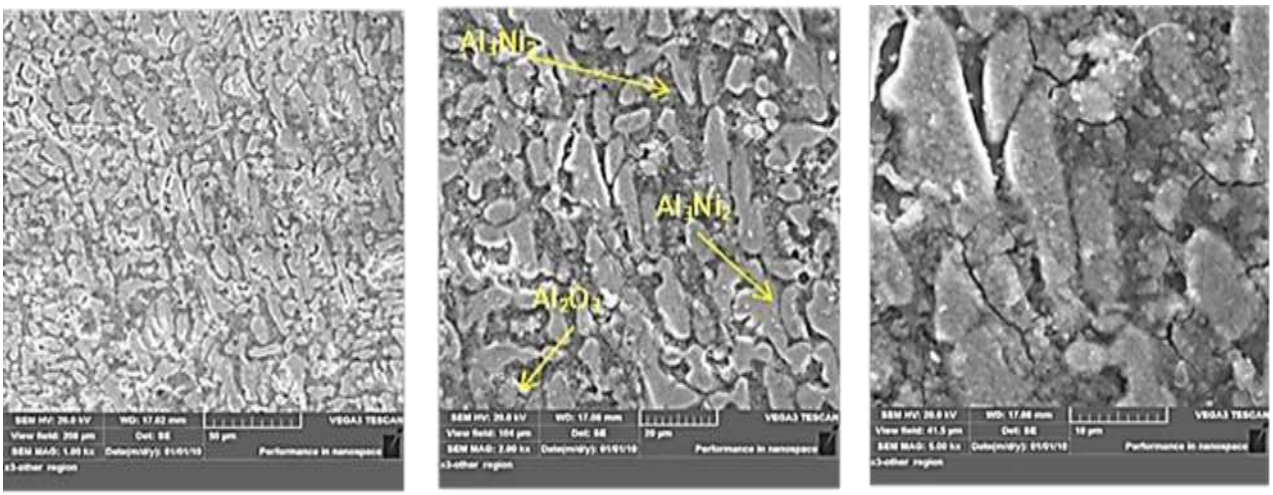

Fig. 4: SEM images of etched Al-20%Ni-8%Al_2O_3 alloy with different magnification.

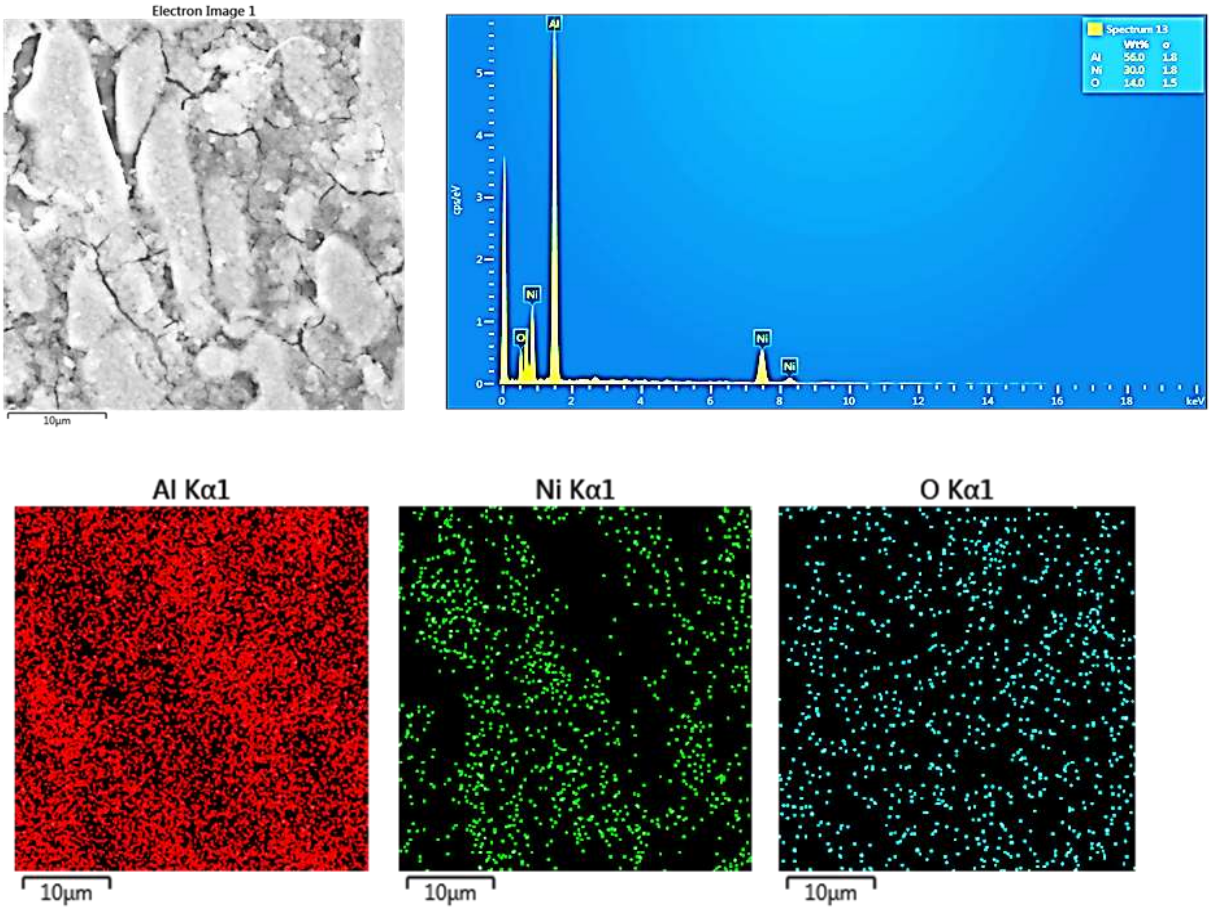

Fig. 5: EDS Spectrum analyses of Al-20%Ni-8%Al_2O_3 alloy.

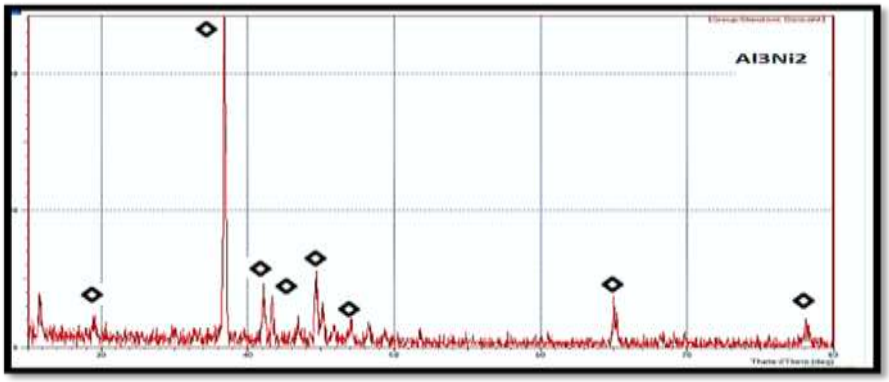

Fig. 6: XRD patterns of Al-20%Ni alloy.

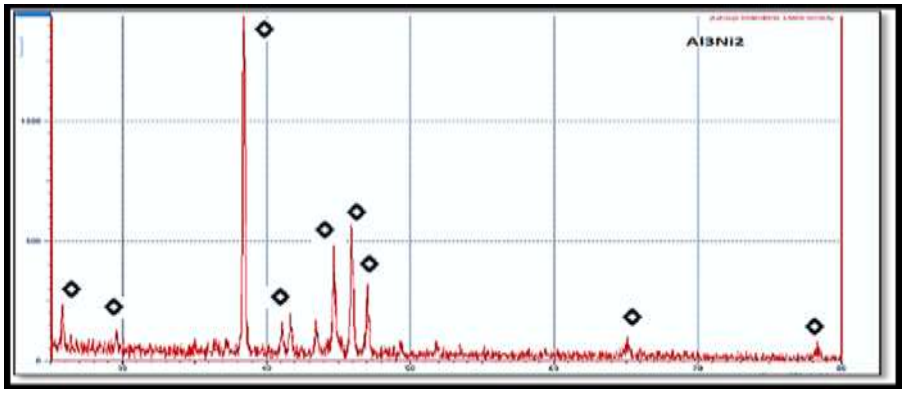

Fig. 7: XRD patterns of Al-20%Ni-8%Al_2O_3 alloy

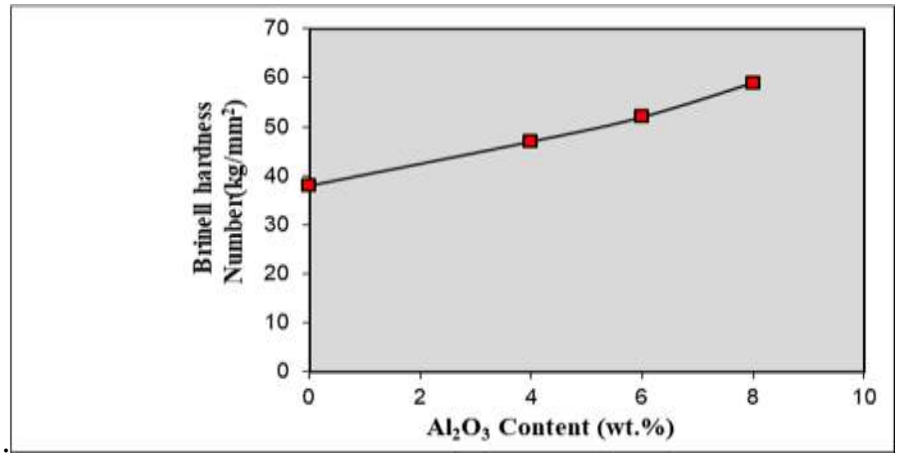

Fig. 8: Influence of Al_2O_3 content on the hardness of Al-20%Ni alloys.

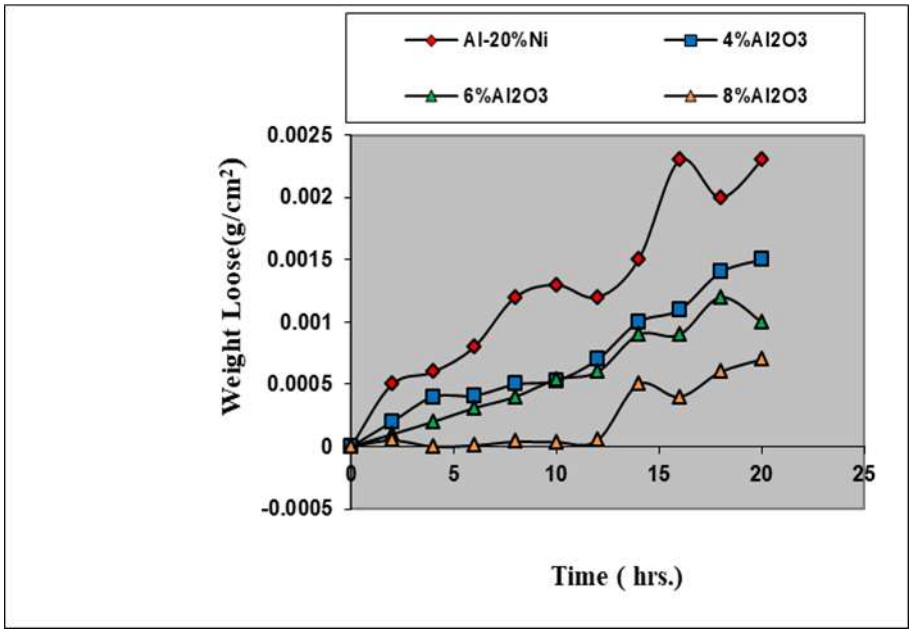

Fig 9: Effect of immersion time on the general pure corrosion in 3.5% NaCl solution of base alloy and composite

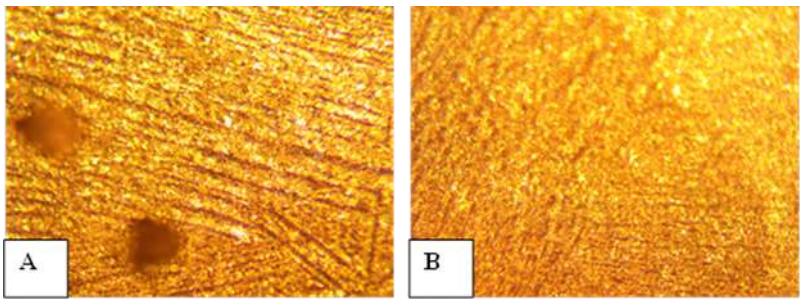

Fig. 10: Microstructure of base alloy after general corrosion test in 3.5% NaCl after immersion time (50 hours.): (a) Al-20%Ni, (b) Al-20%Ni-8%Al_2O_3.

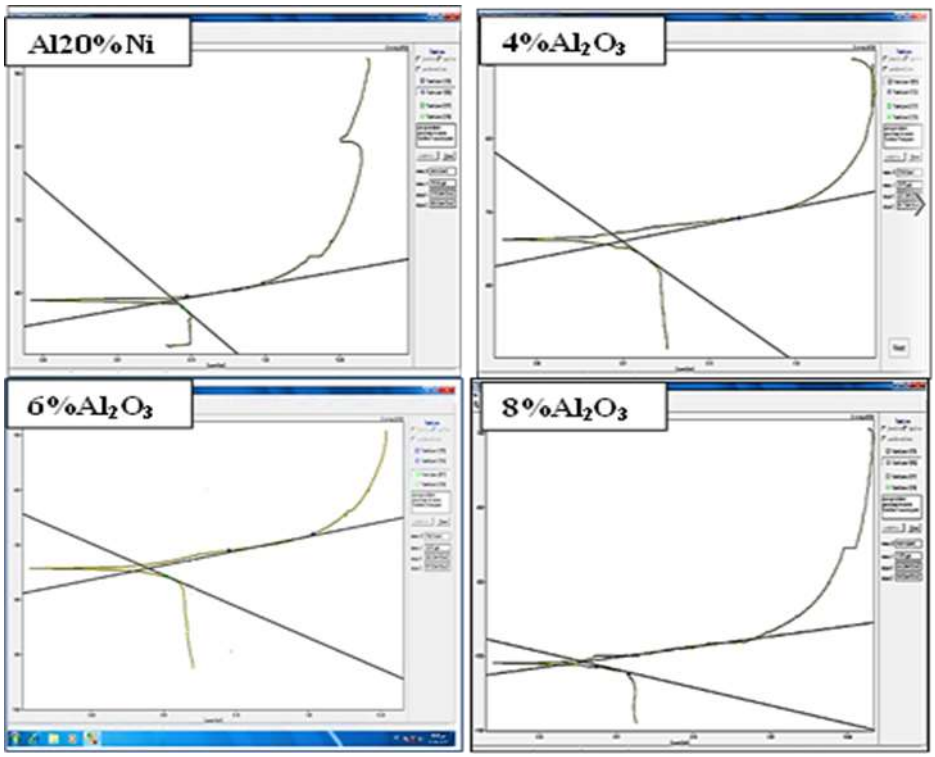

Fig. 11: Polarization curve for Al-20%Ni alloy and composite specimens in 3.5%NaCl solution

Table 4: Corrosion potential (Ecorr.), and Corrosion Current (µA) for Al-20%Ni with and without Al_2O_3 in . 3.5%NaCl

Alloys	***Icorr.*** ***µA***	***Ecorr.*** ***mV***
Al-20Ni	59.04	-809.8
Al-20Ni+4Al_2O_3	9.75	- 739.6
Al-20Ni+6Al_2O_3	6.11	- 742.8
Al-20Ni+8Al_2O_3	3.72	-1007.6

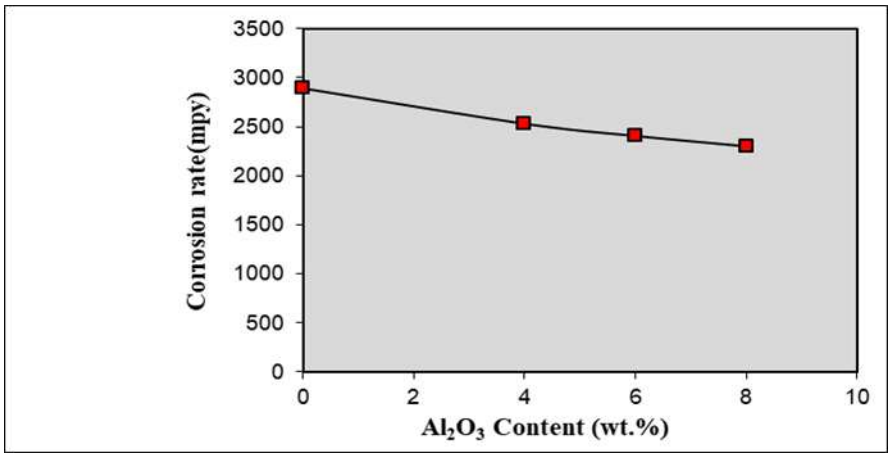

Fig. 12: Effect of Al_2O_3 content on the corrosion rate of Al-20%Ni alloys.

From previous diagrams, the corrosion rates of all the reinforced composites are lower than that of the base metal. The reason behind this is the existence of nickel within the matrix which promotes a superior resistance against corrosion to the whole composite. Moreover, the corrosion rate gradually reduces with increasing the Al_2O_3 reinforcement. This was attributed to the appropriate formation of the passive oxide layer from Al_2O_3 distribution of particles within the matrix. Therefore, surfaces would become more electrochemically passive and this acted as a corrosion-proof. The maximum enhancement in the corrosion protection was found for the composite with 20% Ni and 8% Al_2O_3 where the corrosions rate is decreased by 18.2%.

Erosion–Corrosion Results

Fig. 13 indicates the results of erosion-corrosion of base alloy (Al-20%Ni) and composite samples in slurry solution (3.5wt% NaCl with 1% SiO_2) after an exposure times of 60 hours. at a 2-hour cycle at an impact angle of 90°. It is evident that the curves are fluctuated and the reason behind this fluctuating is of the repeated building and fracture of the protective surface layer. In case of the formation of this layer on the alloy's surface, the erosion-corrosion rate will decrease, whereas, the erosion-corrosion rate will increase as soon as the protective surface layer breaks down. This breaking down depends upon the impact force and the value of adhesion on the surface of the alloys.

At the first time of immersion in the corrosive solution, the rate of corrosion was expected being higher due to the simplicity of removing the created corrosion and the incidence of a new metal surface to be in contact with the corrosive media. In addition, the area covered by deformed zones, produced by the impact of erodent, at the impact location on the surface of the specimen increased with increasing the exposure time at a constant speed of slurry [39].

The composite sample containing 8% Al_2O_3 has the lowest erosion-corrosion rate comparing with base sample (Al20%Ni)**.** This is consistent with the results of researcher Gasem, et al. [40] as they too have noticed that the amounts of pit initiation location increases with the volume fraction of the reinforcement in composite material (Al 6061 –Al_2O_3).

The existence of hard Al_2O_3 particles within the matrix of Al20Ni alloy which has more resistance to erosion-corrosion than the matrix. In addition to this, the silica particles bombardment of the surface increases the metal surface hardness due to the deformation and hardening of the surface. From Fig. 13 it is seen that the erosion-corrosion rate in unit (g/ hr) increases continuously with the exposed time as a result of mechanical effect of pure erosion and electrochemical effect on the corrosive medium. The combined effect of sand in the slurry will lead to pitting corrosion [41]. Das et al [42] indicated that the rate of wear was considerably higher at a normal incidence angle (impact angle 90°) and at a higher speed within the sand slurry media in comparison with that occurring at a lower speed and a smaller incidence angle. The interface between aluminum alloys and solid particulates in the composite materials had a great role in the material elimination process under the synergistic effect of erosion and corrosion.

Conclusions

This study optimized the composites fabricated from 4% Ni and 4, 6, & 8% of Al_2O_3 particle as a reinforcement within the base matrix of pure aluminum using stir casting. The hardness of the Al 20% Ni matrix composites showed increasing trend with increasing the content of Al_2O_3; a maximum increase of 55% was obtained for samples fabricated from 8% Al_2O_3 composite. There was a noticeable decrease in the general corrosion rate or weight loss rate of the composites compared with to pure Al owing to the existence of Ni. Furthermore, the increase in Al_2O_3 content decreased the general corrosion rate in 3.5 wt% NaCl solution for 20 hours at a 2-hour cycle. The corrosion rate or weight loss rate increased continuously with the immersion time for base alloy and composite specimens. The erosion-corrosion rate in slurry solution (1 wt.% SiO_2) in 3.5 wt% NaCl solution is decreased with the addition of Al_2O_3 particles by 14%, 20%, and 26% for specimens of 4, 6, & 8% Al_2O_3, respectively. In erosion–corrosion media, the removal of material was attributed to the combined effect of corrosion and erosion; therefore, the weight loss rate was significantly higher.

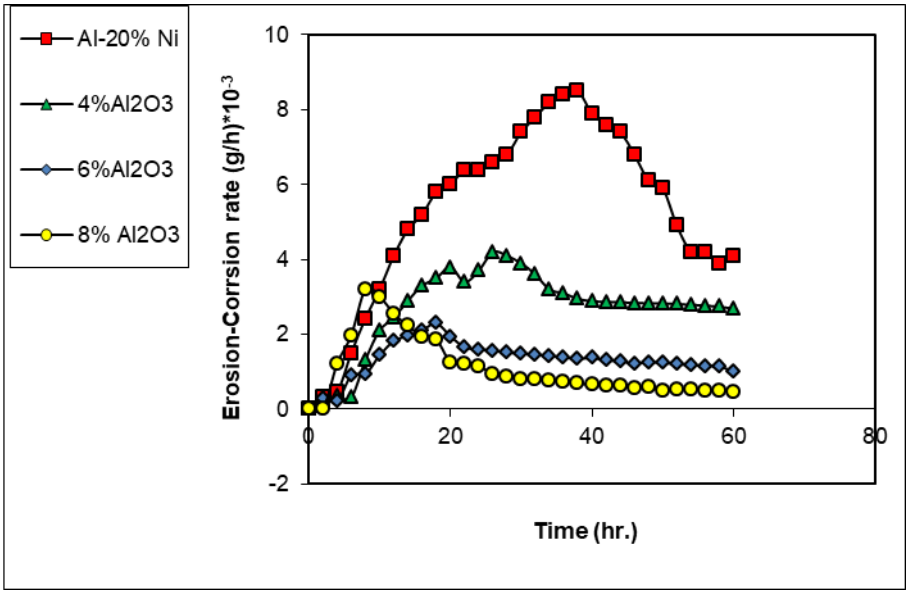

Figure 13: Erosion-corrosion rate test in the slurry solution (1wt% of SiO_2 in 3.5% of NaCl solution) of base alloy and composite samples at an impact angle of 90º

References

[1] A.B. Gurcan, T.N. Baker, Wear behaviour of AA6061 aluminium alloy and its composites, Wear, 188 (1995) 185-191.

[2] S. Ozden, R. Ekici, F. Nair, Investigation of impact behaviour of aluminium based SiC particle reinforced metal–matrix composites, Composites: Part A, 38 (2007) 484-494.

[3] G. Mahajan, N. Karve, U. Patil, P. Kuppan, K. Venkatesan, Analysis of microstructure, hardness and wear of Al-SiC-TiB_2 hybrid metal matrix composite, Indian J. Sci. Tech., 8 (2015) 101-105.

[4] P.C. Yih, D.D.L. Chung, Powder metallurgy fabrication of metal matrix composites using coated fillers, Inter. J. Powder Metall., 31 (1995) 355-340.

[5] M. Asif, K. Chandra, P.S. Misra, Development of aluminum based hybrid metal matrix composites for heavy duty applications, J. Minerals Mater. Chara. Eng., 10 (2011) 1337-1344.

[6] D. Sujan, Z. Oo, M.E. Rahman, M.A. Maleque, C.K. Tan, Physio-mechanical properties of aluminum metal matrix composites reinforced with Al_2O_3 and SiC, Intr. J. Eng. Appl. Sci., 6 (2012) 288-291.

[7] M.A. Khairia, S. Hassan, A.S. Alwan, Study of corrosion resistance of aluminum alloy 6061/SiC composites in 3.5% NaCl solution, Inter. J. Mater. Mech. Manuf., 3 (2015) 31-35.

[8] A. Włodarczyk-Fligier, M. Adamiak, L.A. Dobrzański, Corrosion resistance of the sintered composite materials with the EN AW-AlCu4Mg1(a) alloy matrix reinforced with ceramic particles, J. Achiev. Mater. Manuf. Eng., 42 (2010) 120-126.

[9] B.P. Dileep, V.R. Kumar, M. Prashanth, M.V. Phanibhushana, Effect of Zinc coating on Mechanical Behavior of Al 7075, Appl. Mech. Mater., 592-594 (2014) 255-259.

[10] E. Bayraktar, D. Katundi, Development of a new aluminium matrix composite reinforced with iron oxide (Fe_3O_4), J. Achiev. Mater. Manuf. Eng., 38 (2010) 7-14.

[11] H.X. Guo, B.T. Lu, J.L. Luo, Interaction of mechanical and electrochemical factors in erosion-corrosion of carbon steel, Electrochim. Acta, 51 (2005) 315–323.

[12] A. Neville, F. Reza, S. Chiovelli, T. Revega, Assessing metal matrix composites for corrosion and erosion-corrosion application in the oil sands industry, Corrosion, 62 (2006) 657-675.

[13] J.F. Flores, A. Neville, Materials selection in the oil sands industry based on materials degradation mechanisms, Explor. Prod. Oil Gas Rev., 7 (2009) 42–45.

[14] R. Llewellyn, Resisting wear attack in oil sands mining and processing, CIM Bull., 90 (1997) 75-82.

[15] B.R. Tian, Y.F. Cheng, Erosion-Corrosion of hydro transport pipes in oil sand slurries, Bull. Electrochem., 22 (2006) 329-335.

[16] M. Schorr, B. Valdez, J.D. Ocampo, Erosion-corrosion in industrial steam turbines, Mater. Perform., 48 (2009) 62-65.

[17] M. Schorr, B. Valdez, R. Zlatev, Erosion-corrosion in phosphoric acid production, Mater. Perform., 49 (2010) 56-59.

[18] A.M.F. Carter, Erosion, corrosion, and abrasion of material-handling systems in the mining-industry, J. S. Afr. Inst. Min. Metall., 86(1986) 235-242.

[19] F. Reza, corrosion and erosion-corrosion behavior of materials used for oil sands applications, PhD thesis, Herriot-Watt University, UK, 2005.

[20] S. Das, D.P. Mondal, R. Dasgupta, B.K. Prasad, Mechanisms of material removal during erosion-corrosion of an Al-SiC particle composite, Wear, 236 (1999) 295-302.

[21] D. López, J.P. Congote, J.R. Cano, A. Toro, A.P. Tschiptschin, Effect of particle velocity and impact angle on the corrosion-erosion of AISI 304 and AISI 420 stainless steels, Wear, 259 (2005) 118-124.

[22] I.M. Hutchings, Wear by Particulates, Chem. Eng. Sci., 42 (1987) 869-878.

[23] G.L. Sheldon, I. Finnie, Mechanism of material removal in erosive cutting of brittle materials, J. Eng. Ind., 88 (1966) 393-399.

[24] J. Xie, A.T. Alpas, D.O. Northwood, The role of heat treatment on the erosion-corrosion behavior of AISI, 52100 steel, Mater. Sci. Eng. A, 393 (2005) 42-50.

[25] X. Hu, A. Neville, The electrochemical response of stainless steels in liquid-solid impingement, Wear, 258(2005) 641-648.

[26] E.A.M. Hussain, M.J. Robinson, Erosion-corrosion of 2205 duplex stainless steel in flowing seawater containing sand particles, Corros. Sci., 49 (2007) 1737-1754.

[27] M.B. Abuzriba, R.A. Dodd, F.J. Worzala, J.R. Conrad, Technical note: wear corrosion: separation of the components of corrosion and wear, Corrosion, 48 (1992) 2-4.

[28] N. Latona, P. Fetherston, A. Chen, K. Sridharan, R.A. Dodd, Wear- corrosion comparisons of passivating vs non-passivating alloys in aerated 3.5% aqueous solutions of sodium chloride, Corrosion, 57 (2001) 884-888.

[29] J.A. Bester, A. Ball, The performance of aluminum alloys and particulate reinforced aluminum metal matrix composites in erosive-corrosive slurry environments, Wear, 162-164 (1993) 57-63.

[30] K.P. Cooper, P.L. Slebodnick, K.E. Lucas, E.A. Hogan, microstructural inhomogeneities and sea water corrosion in laser- deposited Ti-6Al-4V alloy matrix/carbide particulate composite surfaces, J. Mater. Sci., 33(1998) 3805-3816.

[31] W.S. Hwang, H.W. Kim, Galvanic coupling effect on corrosion behavior of al alloy-matrix composites, Met. Mater. Int., 8 (2002) 571-575.

[32] A.H. Haleem, N.F. Kadhem, The Effect of SiC addition on AlNi compact mechanical properties produced via powder metallurgy, J. Uni. Babylon Eng. Sci., 27 (2019) 105-118.

[33] B.P. Dileep, V.b. Ravikumar, H.R. Vital, Mechanical and corrosion behavior of Al-Ni-SiC metal matrix composites by powder metallurgy, Materialstoday Proceed., 5 (2018) 12257-12264.

[34] ASTM Volume 03.02 Corrosion of Metals, Wear and Erosion, ASTM, 1988.

[35] https://www.researchgate.net/figure/Schematic-for-device-used-at-corrosion-erosion-wear-testing-In-the-figure-the-acronyms_fig1_288499450

[36] P.K. Dalai, A. Senapati, Experimental investigation and analysis of process parameter in machining of aluminum based metal matrix composite, Inter. J. Eng. Sci. Rese. Tech., 3 (2014) 94-102.

[37] L. Sankar, R. Srinivasan, P. Viswanathan, R. Subramanian, Comparison study of Al-fly ash composite in automobile clutch plates, Inter. J. Emerging trends Eng. Develop., 3 (2013) 77-91.

[38] L.L. Shreir, R.A. Jarman, G.T. Burstein, Corrosion-Metal/environment reaction, Third ed., Vol.1, Oxford, Butterworth-Heinemann, LTD, 1993.

[39] Z. Brodarac, Z.P. Mrvar, J. Medved, P. Fajfar, Local squeezing casting influence on the compactness of $AlSi_{10}Mg$ alloy casting, Metalurgija, 46 (2007) 29-35.

[40] Z. M. Gasem, A.M. Al-Qutub, Corrosion behavior of powder metallurgy aluminum alloy 6061/ Al_2O_3 metal matrix composites, The 6th Saudi Engineering Conference, KFUPM, Dhahran, December 5 (2002) 271-280.

[41] H.H. Abd, Behavior of different welded joints for Al-alloy (6061-T6) in erosive- corrosive environments, MSc. thesis, University of Technology, Iraq, 2012.

[42] S. Das, D.P. Mondal, R. Dasgupta, B.K. Pasad, Mechanism of material removal during erosion-corrosion of an Al-SiC particle composite, Wear, 236 (1999) 295-302.